Spec. Publ. geol. Soc. S. Afr., 7 (1983), 351–363

THE "DIG-OUT" OF A FERROCHROMIUM FURNACE

by

A. WEDEPOHL and N.A. BARCZA

National Institute for Metallury, Private Bag X3015, Randburg 2125, S. Africa.

ABSTRACT

A 48 MVA submerged-arc furnace, which has been used for the production of high-carbon ferrochromium from chromite ore of the Bushveld Complex, was excavated approximately one month after it had been switched off.

A mineralogical study was made of samples from various regions of the furnace so that the reduction mechanism involved in the reduction and smelting of South African chromium ore under actual plant conditions would be elucidated. The ultimate purpose of the study was an improvement of the efficiency of the process by the application, wherever possible, of the knowledge gained.

The conclusions drawn from the profiles of chromite particles in different stages of reduction, which were based on electron-microprobe analyses, were of particular interest. The profiles showed that the order of reduction of oxides in chrome spinel to metallic phases is different in local ores from that in other ores.

The role of silica in the reduction mechanism and the phases in which residual chromium is found are also discussed.

INTRODUCTION

The ferro-alloy industry in South Africa has been characterised in recent years by a steady increase in the size of the electric-smelting furnaces used from 9 MVA units up to large units of 81 MVA. The largest furnace used so far in this country for the production of high-carbon ferrochromium is a 48 MVA unit. The metallurgical and electrical operation of these large furnaces was initially fraught with problems, mainly as a result of lack of experience in controlling the process. This situation gave rise to requests from the ferro-alloy industry that have led to a number of applied research projects at the National Institute for Metallurgy (NIM) on the computer control of furnaces (Sommer).

It was soon realised that, although the high-temperature chemistry of the reduction of chromite ore by carbon was reasonably well understood, very little was known about the overall reduction and smelting behaviour of the burden in an industrial electric furnace. An investigation of the contents of a 48 MVA furnace that had been used for the production of high-carbon ferrochromium became possible when such a furnace was switched off so that it could be rebuilt. The planning of the excavation or "dig-out" was carried out jointly by the plant concerned (Ferrometals in Witbank), by Samancor Management Services and by NIM. The furnace was divided into vertical and horizontal sections, and the samples were taken and labelled according to a special code. The sampling was supervised by NIM and took place one month after the furnace had been switched off. Macroscopic observations of the various zones of interest were made during the excavation, especially in the former high-temperature regions close to the three self-baking graphite electrodes, and a photographic record was kept. A detailed report on this dig-out has been published (Wedepohl).

The numerous samples taken from the various regions of the furnace provided a unique opportunity for a mineralogical study that, it was hoped, would elucidate the reduction and smelting mechanisms in the environment of a production furnace. This improved understanding of the process was considered to be an essential part of the overall metallurgical control of the operation since chromite ores from the Bushveld Complex are known to behave somewhat differently from other chromite ores. Such differences were thought to be related to their higher iron and lower aluminium and magnesium contents which make the local ores less refractory.

Work that has been done on a macroscopic scale indicates that silica has a two-fold function: as a flux for smelting, and as a participant in the reduction process. However, this latter role has not yet been elucidated, and it was hoped that the study would also contribute to an understanding of this phenomenon. A further purpose of the mineralogical study was the determination of the form of residual chromium in the slag and the phases in which it is present.

The furnace that was excavated has an internal depth of 4,3 m and an internal diameter of 10,9 m. The electrical current is supplied by three symmetrically positioned Söderberg electrodes, each of which has a diameter of 1,55 m. Fig. 1 shows the upper surface of the furnace burden near the start of the dig-out.

A submerged-arc furnace is operated at high current and relatively low voltage. A typical current for each electrode is about 100 kA, and typical potentials between the electrodes are of about 150 V.

Figure 1
The furnace at the start of the dig-out, showing the three Söderberg electrodes and the top of the burden (part of which had already been removed).

The following raw materials had been fed into the furnace before its shut-down:

1. coke breeze as the carbonaceous reducing agent,
2. pure quartzite, with a mixture of dolomite, lime and serpentine as the fluxing materials, and
3. chromium ore from various parts of the Bushveld Complex.

The quantities of the flux ingredients are chosen to control the physicochemical properties of the slag, i.e. liquidus temperature, viscosity and conductivity. These properties of the slag depend largely on its basicity, i.e. $(CaO + MgO)/SiO_2$.

The chromium ore has the following typical composition, in approximate percentages by mass: Cr_2O_3 40, Fe_2O_3 5, FeO 19, MgO 12, Al_2O_3 14, SiO_2 6 and CaO 1.

The major gangue minerals in the ore are olivine, pyroxene, serpentine and chlorite. However, the quantity and constitution of the gangue material depend on the place of origin of the ore (De Waal).

INVESTIGATIONAL PROCEDURE

Representative samples were taken from the region surrounding each of the three electrodes from positions chosen in such a way that the samples would be likely to show differences depending on the distance of the sample from the electrode (i.e. towards the wall of the furnace) and depending on the level of the sample in relation to the top of the burden.

The samples were investigated by optical means, during which both polished sections and thin sections were examined.

X-ray diffraction photographs of the various phases were taken, but particular metallic phases were occasionally difficult to identify since they sometimes occured in very small quantities within other phases. The carbides posed another difficulty since the X-ray diffraction patterns of carbides tend to be very weak and their *d*-values tend to overlap. However, where difficulties were encountered, metallic phases were identified by a comparison of their electron-microprobe analyses with the constitution of phases in the system iron–chromium–carbon (Griffing) and iron–chromium–silicon–carbon (Wethmar). Difficulties were also encountered with the exact matching of X-ray diffraction patterns for the slag phases. In general, the patterns indicated the general type of phase (e.g. pyroxene, spinel, etc.), but the precise constitution of the phase could be found only from quantitative electron-microprobe analyses.

The electron-microprobe analyses conducted included qualitative analyses by use of energy-dispersive spectroscopy (EDS) and quantitative or semiquantitative analyses on all the slag and metallic phases that were examined.

The two most important sets of electron-microprobe analyses were quantitative analyses of the metallic phases in samples from several regions of the furnace and analyses of altered chromite particles. The latter were conducted and used as follows.

Profiles of cation percentages by mass across chromite particles in various stages of alteration were drawn from the electron-microprobe analyses of points along a line passing from one edge of a particle to the other edge through its centre. The points at which the analyses were done were 20 to 30 μm apart, and they were analysed for nine elements (chromium, iron, aluminium, magnesium, silicon, calcium, titanium, sulphur and carbon). Not all the elements were plotted in the profiles. The titanium and sulphur values were not plotted since they were at all times low, and the carbon values were omitted since, although qualitatively informative, they were considered to be quantitatively inaccurate. In general, the values plotted can be regarded as semiquantitative since the same standards were used throughout the profiles and the values can be regarded as accurate to within about two per cent. This does not apply to the metallic blebs for which

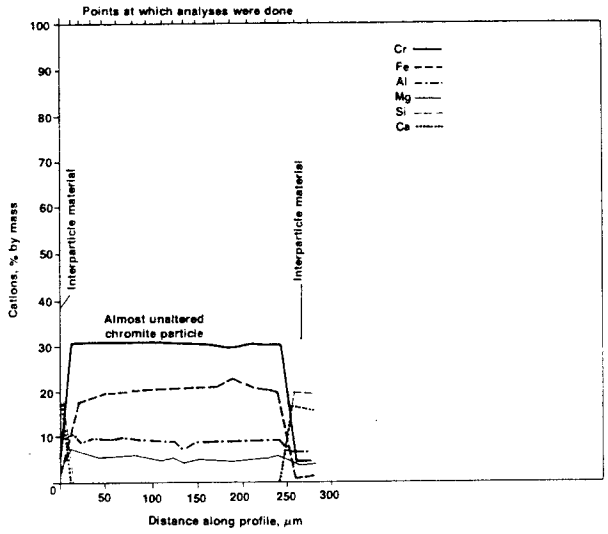

Figure 2
Type A PAC particle.

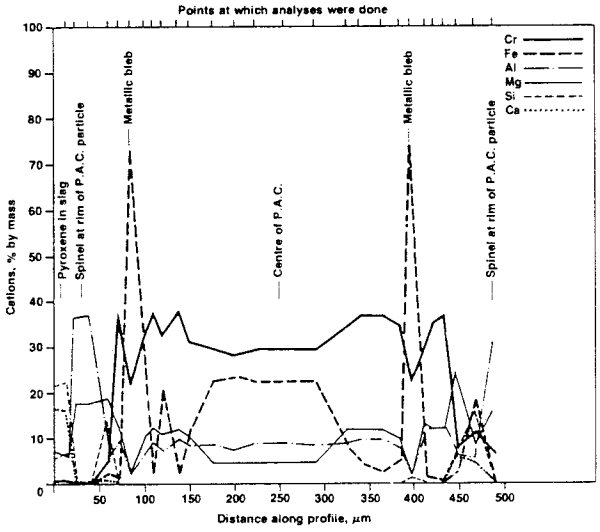

Figure 3
Type B PAC particle.

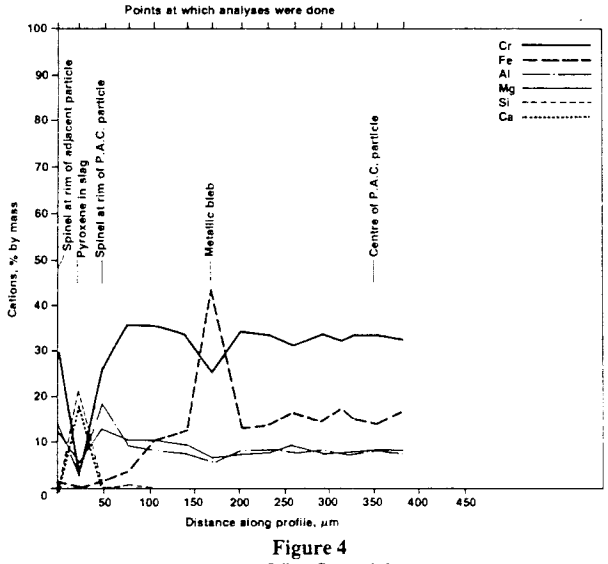

Figure 4
Type C PAC particle.

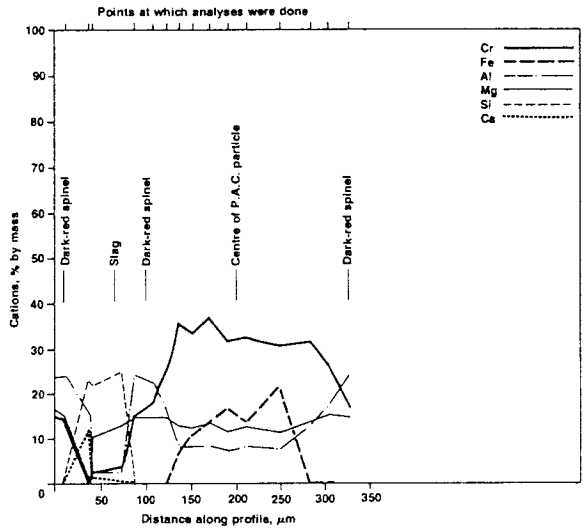

Figure 5
Type D PAC particle.

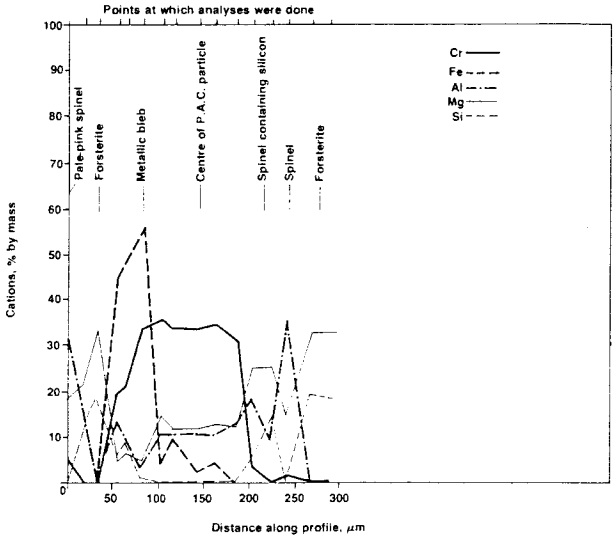

Figure 6
Type E PAC particle.

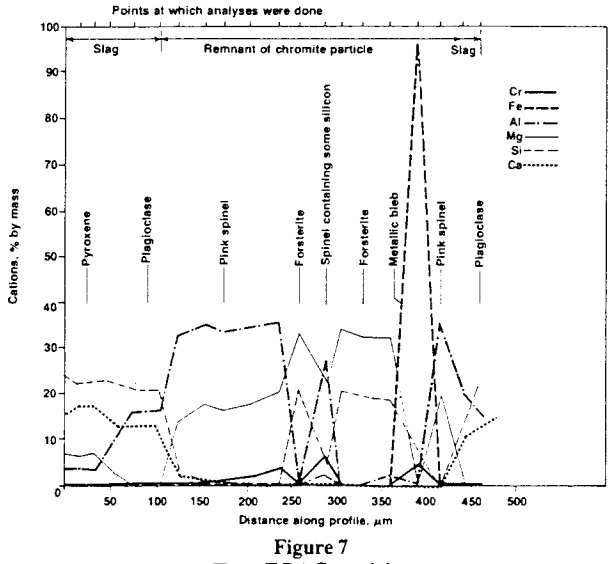

Figure 7
Type F PAC particle.

the accuracy was approximately ten per cent since metallic standards were not used. The plotted profiles are shown in Figs. 2 to 9.

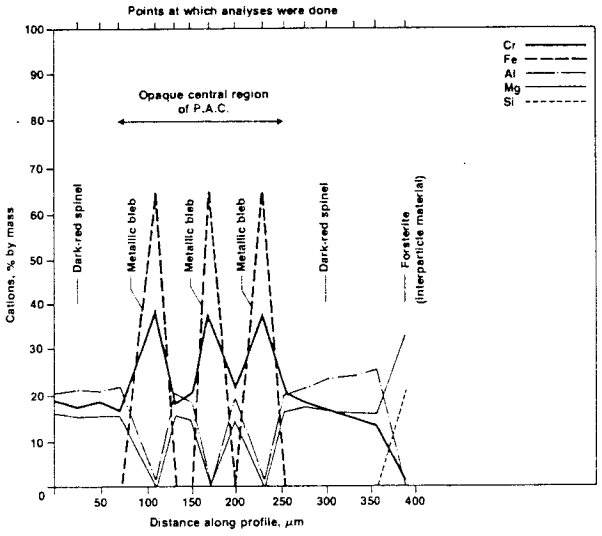

Figure 8
Type G PAC particle.

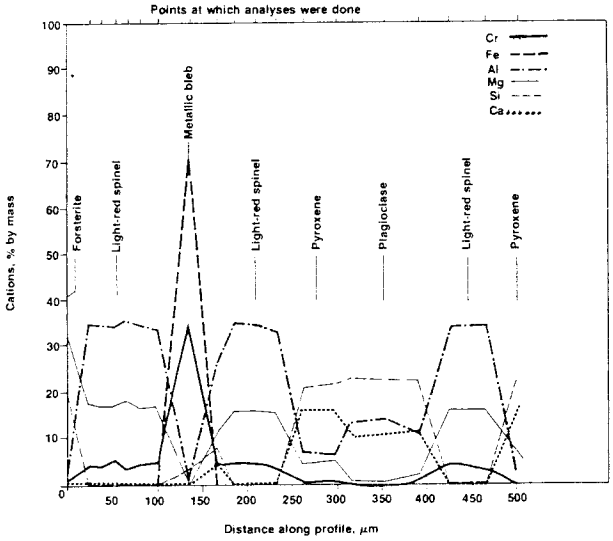

Figure 9
Type H PAC particle.

GENERAL OBSERVATIONS

The samples of slag tended to be porous, particularly those from higher positions in the furnace. This is to be expected since, throughout the process, gases, particularly carbon monoxide (a product of the reduction processes taking place in the furnace), are continuously flowing upwards through the burden to the surface. Typical reduction reactions are as follows:

$$FeO + C \rightarrow Fe + CO \text{ or } 3FeO + 4C \rightarrow Fe_3C + 3CO$$

$$Cr_2O_3 + \frac{27}{7}C \rightarrow \frac{2}{7}Cr_7C_3 + 3CO$$

The colour of the slags when viewed with the naked eye was grey in samples taken from positions near the tips of electrodes and red or orange in samples taken from near the walls of the furnace and the surface of the burden.

PHASES IN THE SAMPLES

The phases found in all the samples in varying amounts were forsterite, plagioclase, pyroxenes, spinels (including chromite particles in various stages of alteration) and metallic phases (including metal carbides).

Forsterite

When forsterite (Mg_2SiO_4), which was present in small amounts, occurred together with black pyroxene, it con-

tained chromium — from one to two per cent by mass. However, most of the forsterite present contained no chromium and was colourless and transparent.

Plagioclase

The physical characteristics of the plagioclase, i.e. anorthite ($CaAl_2Si_2O_8$), seemed to have been influenced by the surrounding conditions. Perhaps the presence of a reducing atmosphere had exerted some effect. The crystals, which were clear and transparent, almost always appeared together with opaque clinopyroxene. The crystals were tabular in form and often had a characteristic parting down the middle parallel to their long axes. Fractures at right-angles to these axes were also typical. Where crystals of plagioclase and pyroxene were well resolved, they frequently formed a fan-shaped pattern. All these characteristics are illustrated in Fig. 10.

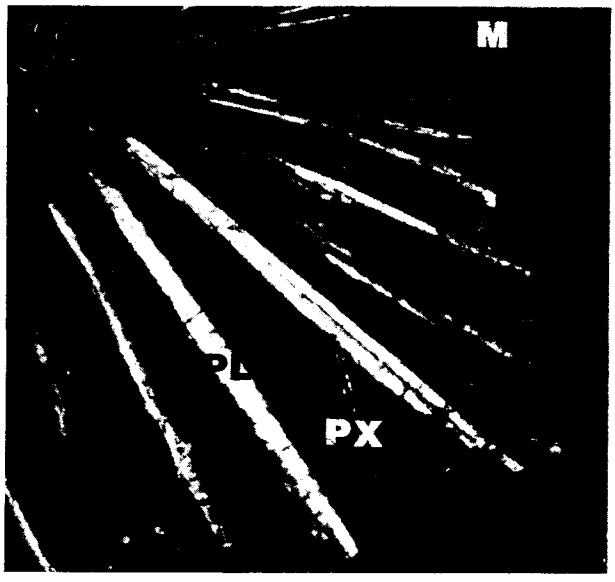

Figure 10
Exsolution crystal of anorthite (PL) and pyroxene (PX) showing the typical characteristics of these phases.
Transmitted light, 160 ×. Width of figure ≡ 0,5 mm.

The X-ray diffraction pattern of this phase was similar, but not identical, to any standard plagioclase pattern.

Electron-microprobe analyses showed that the phase contained slightly less aluminium, and correspondingly more silicon, than ideal anorthite. A small amount of magnesium was observed to have replaced calcium in the lattice.

Pyroxenes

The clinopyroxenes occurred in several forms, all of which, being rich in aluminium, consisted of a solid solution of Tschermak molecule ($CaAl_2SiO_6$) and diopside ($CaMgSi_2O_6$).

One range of pyroxenes that usually occurred as exsolution crystals together with plagioclase varied from white to grey to black when viewed with the stereomicroscope. All these pyroxenes varied from slightly to completely opaque.

The aluminium varied from 3,64 to 10,45 per cent by mass. The latter value was for a black pyroxene crystal and approximates the maximum amount of Tschermak molecule that can be dissolved in diopside, which was found to be less than 40 mole per cent at atmospheric temperature and pressure (Neufville).

The white pyroxene contained no chromium at all but the black pyroxene had a chromium content of 2,33 per cent and also contained some sulphur. It was always accompanied by dentritic crystals of (Cr,Mn)S. Fig. 11

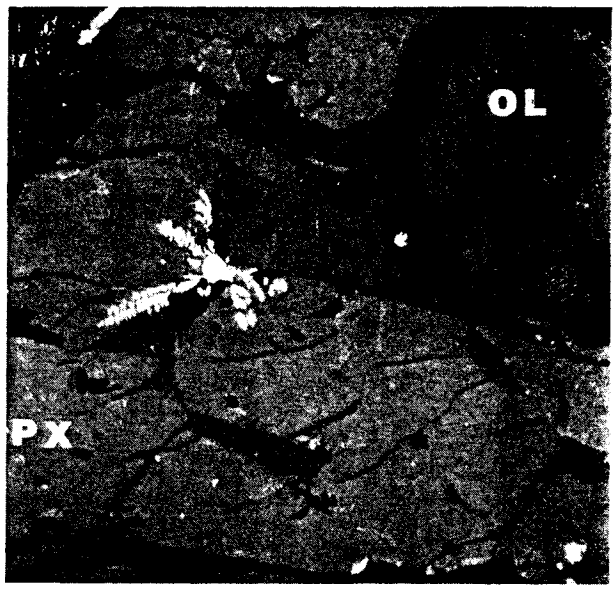

Figure 11
Dentritic crystal of (Cr,Mn)S growing in a crystal of black pyroxene. To the right of the dentritic crystal is a cracked olivine crystal (OL).
Reflected light, 200 ×. Width of figure ≡ 0,4 mm.

shows such a dendritic crystal in a large black pyroxene crystal. The cracked crystal to the right of the dendritic crystal is forsterite. The position of the pyroxene crystal was within a tongue of dark material in a sample of slag taken from a position near the furnace wall. The material consisted of black pyroxene and chromium containing forsterite which was surrounded by a thin coat of metallic phase.

The grey pyroxene had a chromium content of between 0 and 2,33 per cent.

The X-ray diffraction patterns for the black, grey and white pyroxenes did not completely correspond to any known pyroxene pattern but, apart from variations in the intensities of their lines, were consistent among themselves.

A transparent, green pyroxene was also observed, the crystal being slightly pleochroic and often cracked. The electron-microprobe analysis showed this green variety to be similar to the other pyroxenes. It had a chromium content of 1,85 per cent chromium but less aluminium than the black pyroxene. The X-ray diffraction pattern fitted that of fassaite reasonably well, although, unlike fassaite, it contained a negligible amount of iron.

Table I gives a comparison between the atomic proportions of the main elements shown by electron-microprobe analysis to be present in the pyroxenes. It should be noted that the atomic proportion of calcium was very nearly equal to one in each case and that the amount of iron was negligible. Traces of titanium, sodium and manganese were also found in the pyroxenes.

TABLE I
Total Atomic Proportions of Cations in Pyroxenes when Oxygen is equal to 6

Colour	Ca^{2+}	Al^{3+}	Mg^{2+}	Cr^{2+}	Si^{4+}	Fe^{2+} and Fe^{3+}
Black	0.94	0.84	0.57	0.10	1.43	0.00
White	0.97	0.33	0.58	0.00	1.84	0.00
Green	0.95	0.43	0.75	0.08	1.70	0.01

In the samples of slag examined, the most commonly observed pyroxenes were white or grey which occurred as exsolution crystals with plagioclase. This combination is referred to as PX/PL. There were occasional small dark

spots that consisted of plagioclase, forsterite and black pyroxene including dendrites.

In active regions, the pyroxene was predominantly of the white variety and, where slag was entrained in reducing agent, the PX/PL was invariably white.

Grey, black and green pyroxenes were found fairly frequently in samples of slag from the less-active regions of the furnace.

Spinels

Both transparent spinels and chromite particles ($A^{2+}B^{3}_{2}+O_4$) are discussed under this heading.

The transparent spinels ranged in colour from colourless through to pale pink, light red, red and dark red; however, orange and deep-orange spinels were also observed in samples of slag. The electron-microprobe analyses showed that, the deeper the colour, the greater the amount of chromium in the spinel. The amount of iron was negligible in all the transparent spinels. The analyses of the light-red and orange spinels were very similar, although the atomic proportion of titanium in the latter was greater than that in the former by a factor of 4,5, a difference that may account for the difference in colour. The amount of titanium present was always very small.

It was noted that the spinels occur in three modes: as remnants of altered chromite particles, having irregular shapes and lying within the framework of the original particle; as rims of chromite particles in an earlier stage of alteration; or as separate euhedral crystals that, presumably, recrystallized out of the slag. Table II gives the atomic proportions of the elements present in the transparent spinels.

TABLE II
Atomic Proportions of Cations in Transparent Spinels when Oxygen is 4, i.e. $A^{2+}B^{3+}_{2}O_4$

Colour	Mg^{2+}	Al^{3+}	Cr^{3+}	Fe^{3+}	Ti^{4+}	Si^{4+}	ΣB^{3+} and B^{4+}
Pale pink	1,075	1,902	0,033	0,006	0,004	0,002	1,95
Orange	1,01	1,83	0,130	0,000	0,027	0,001	1,99
Light red	0,99	1,855	0,141	0,000	0,006	0,006	2,08
Red	1,00	1,840	0,154	0,023	0,006	0,002	2,03
Dark red	1,109	1,314	0,601	0,000	0,008	0,008	1,93

The entire spinel crystals or parts of them were very often anisotropic, probably owing to the distortion of the spinel lattice by the replacement of magnesium and aluminium with other ions, including some silicon.

Chromite

The chromite particles present in various stages of alteration are also classed as spinels. These rounded particles were found throughout the samples of slag and they ranged from approximately 300 to 500 μm.

Eight different stages of alteration could be identified optically. The particles characterising each stage were assigned the letters A to G, which indicate the degree of alteration; for example, A designates almost unaltered chromite particles and G designates particles that have been altered almost completely. These partially altered chromite particles are referred to as PAC particles.

Figs. 12–14 show photomicrographs of PAC particles in ascending order of alteration. It should be noted that the white spots in the photomicrographs taken in reflected light are metallic blebs. The same blebs show up as dark spots in the corresponding photomicrographs taken in transmitted light. The optical descriptions of the eight types of PAC particles are as follows.

Type A

The particles consist of complete opaque, almost unaltered chromite. Metallic blebs occur interstitially in the region of these particles.

Type B

The particles have a transparent rim of red spinel surrounding the opaque centre. The metallic blebs that occur on the outer edge of the opaque centre seem to coincide in position and shape with cracks in the chromite particles, indicating that the particle has been reduced preferentially where there has been easy access for the reducing agent.

Type C

These particles also consist of a transparent rim of red material surrounding an opaque centre. However, it appears that some degree of melting and sintering has taken place by this stage, since these particles have comparatively smooth uncracked surfaces and are often larger than other types of PAC particles. Metallic blebs occur at the outer edge of the opaque central region.

Type D

The particles have smooth surfaces, similar to those of type C, but there are small metallic blebs in the centre of the opaque region rather than at the edge.

Type E

The particles have rims consisting of pale-pink spinel. The central region is still opaque but the metallic blebs in the centre are larger, and are long with rather irregular shapes. They are sometimes joined together as if beginning to coalesce.

Type F

The particles are heterogeneous in appearance and appear to represent the last stages of alteration of a chromite particle. Pink spinel occurs at the edge of the particles and within them. These particles are usually transparent except where there are metallic blebs, but they have occasional rounded, opaque regions (Figs. 13c and d). The electron-microprobe analyses of such regions did not reveal significant differences between them and the transparent regions alongside them. However, there is a suggestion of a very small amount of extra iron in the opaque regions of the spinels, i.e. 0,1 to 0,2 per cent, whereas the electron-microprobe analysis indicates that there is no iron in the transparent spinel alongside it. (It should be noted that the chromite in ores from the USSR is transparent in thin section.) The metallic blebs in these particles vary in size from large to small. They are well rounded, and the larger blebs tend to be in the middle of the particle.

Type G

Particles of this type resemble PAC particles of type E under reflected light. In thin section under transmitted light, the centres are also opaque but the rim of spinel round the particle is dark red rather than pink. The metallic blebs, which are in the central opaque regions of the particles, tend to be larger than the corresponding blebs in PAC particles of type E, and they are long and irregularly shaped.

Type H

PAC particles of type H are very similar to particles of type F in every respect, except that their remnant spinels are light red rather than pale pink.

PAC particles of types A to D were found in samples from all regions of the furnace, although type D seemed less common than the others. However, particles of types E and F were found in the more active regions of the furnace where the residual amount of Cr_2O_3 in the slag is low.

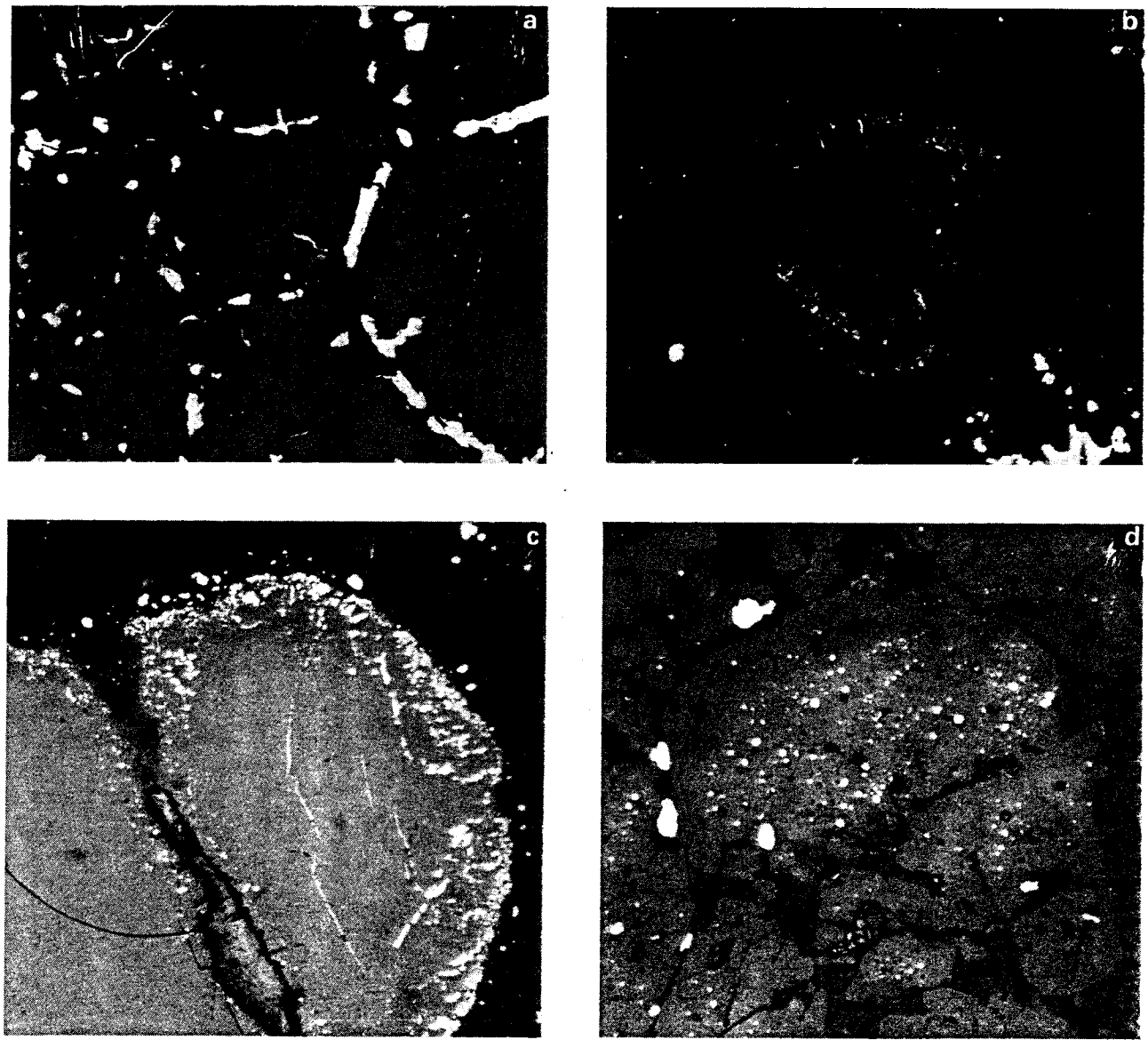

Figure 12

a. A group of type A PAC particles with interstitial metallic blebs.
Reflected light, 160 ×. Width of figure ≡ 0,5 mm.

b. A type B PAC particle surrounded by dark-coloured stag.
Reflected light, 80 ×. Width of figure ≡ 1,0 mm.

c. Two typically large type C PAC particles sintered together. The lighter colour of the particles is also typical. (The circle was made with a diamond needle to mark the position for electron-microprobe analysis.)
Reflected light, 80 ×. Width of figure ≡ 1,0 mm.

d. A group of type D PAC particles with dark coloured slag between them.
Reflected light, 160 ×. Width of figure ≡ 0,5 mm.

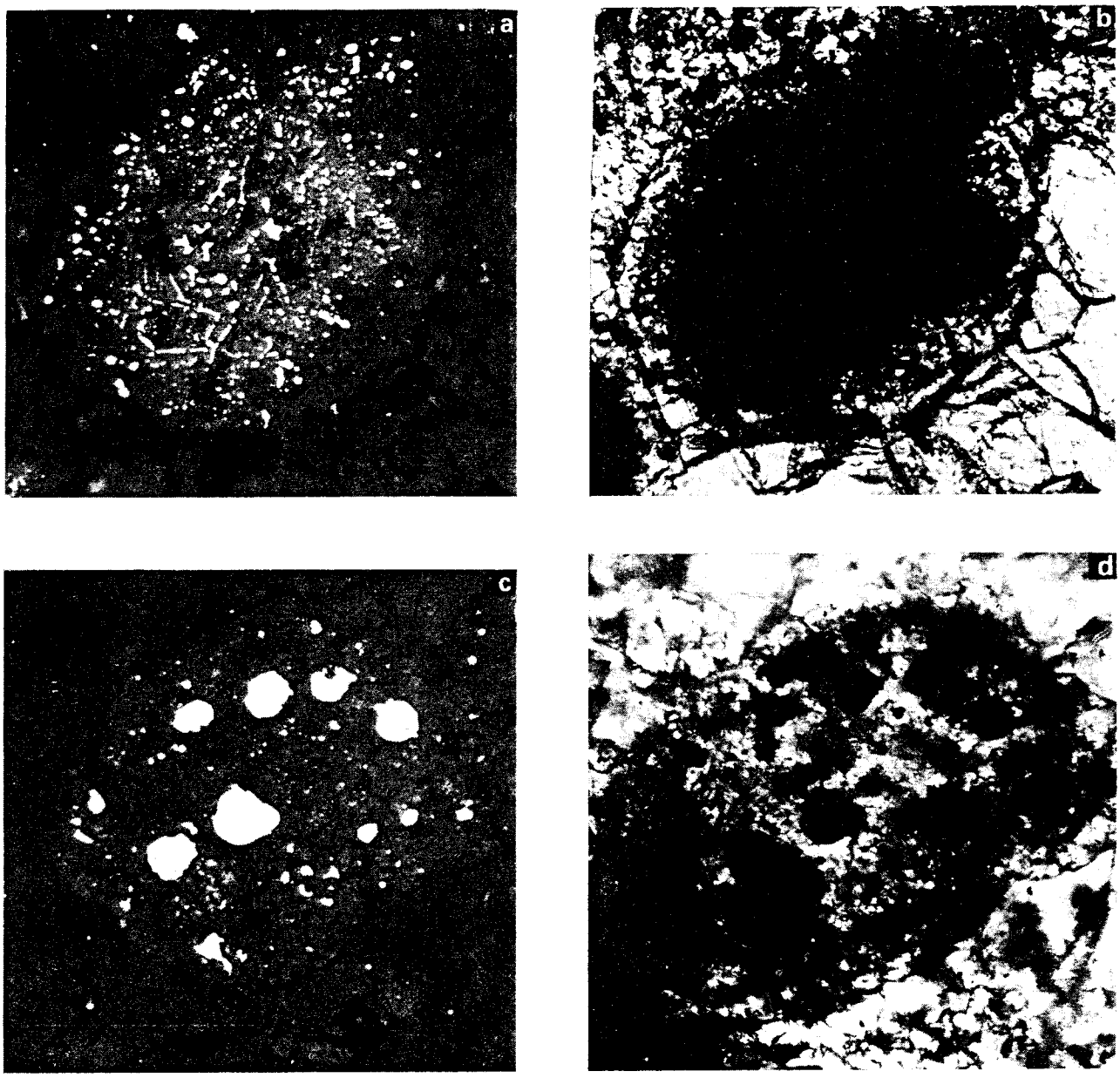

Figure 13

a. A large type E PAC particle in the centre of the photograph, with a small type E PAC particle in the lower left-hand corner. Reflected light, 160 ×. Width of figure ≡ 0.5 mm.

b. The same type E particle as in a. The transparent rim of the PAC particle consists of pale-pink spinel. The large crystals in the slag to the right of and below the central PAC particle are forsterite. Transmitted light 160 ×.

c. A type F PAC particle. The PAC (centre) is surrounded by slag. Reflected light, 160 ×. Width of figure ≡ 0.5 mm.

d. The same type F PAC particle. Note that not all the dark spots are due to the presence of metallic blebs. The residual spinel within the particle is pale-pink in colour. Opaque slag in the lower left-hand corner is PX/PL. Transmitted light 160 ×.

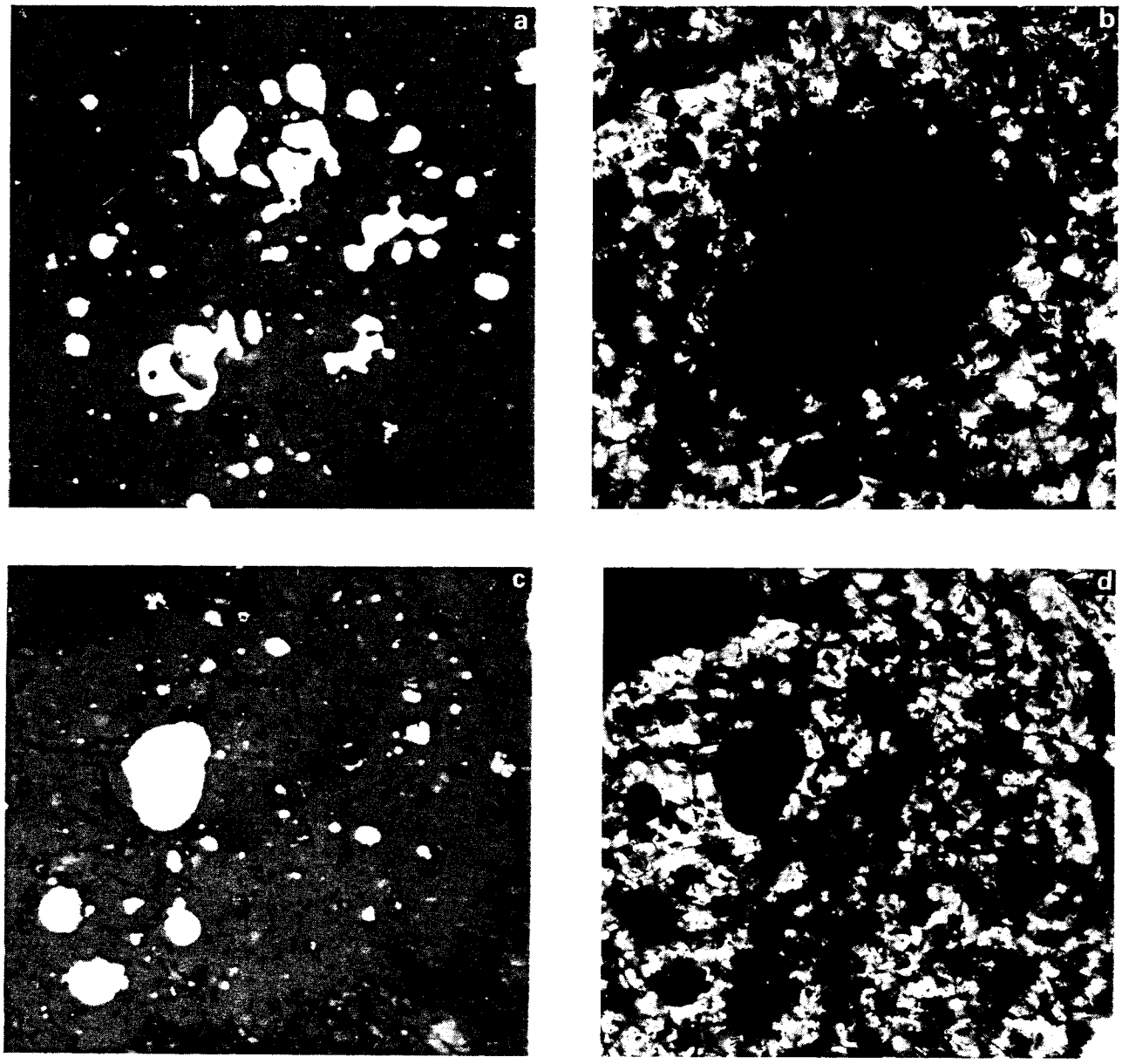

Figure 14

a. A type G PAC particle. The metallic blebs are within the central region of the particle, which is itself better defined in the adjoining photomicrograph.
Reflected light 160 ×. Width of figure ≡ 0,5 mm.

b. The same type G PAC particle as in a. The transparent rim consists of dark-red spinel.
Transmitted light, 160 ×.

c. A type H PAC particle.
Reflected light 160 ×. Width of figure ≡ 0,5 mm.

d. The same type H PAC particle as in c. The residual spinel within the particle is light red.
Transmitted light, 160 ×.

Particles representing several stages of reduction or alteration can be found in one region since, according to tracer tests, there is a constant movement of material within a furnace of this type. PAC particles at a more-advanced state of alteration would have been in an active region for longer than others at a less-advanced state of alteration.

Towards the surface of the burden and towards the outer wall of the furnace, PAC particles of types E and F were replaced by PAC particles of types G and H, respectively. In these regions, the residual Cr_2O_3 in the slag was high according to the chemical analyses.

Metallic Phases

Metallic phases occurred in the section as large areas of coalesced carbides or metal, which sometimes obviously surrounded pieces of reducing agent. Alternatively, they occurred as metallic blebs within PAC particles or as apparently independent blebs. Some blebs were seen to consist of more than one phase.

There were also, occasionally, very small metallic speckles within other minerals, i.e. spinels or forsterite. Those in the latter appeared to be almost pure iron but the electron-microprobe analysis was hampered by the

very small size of the speckles.

Of the several minor metallic phases in the samples, $(Ti,Cr)_3C_2$ was the most common. It is a hard, purple phase and occurred as small euhedral crystals within the main metallic phase. However, the predominant phases were a chromium-rich phase and an iron-rich phase.

The Chromium-rich Phase

This term designates a metallic phase richer in chromium than in iron, or containing approximately equal amounts of chromium and iron with no silicon and an appreciable amount of carbon. This would be the phase $(Cr,Fe)_7C_3$ that was identified from X-ray diffraction photographs as the main metallic phase in the final carbide product from the furnace.

The Iron-rich Phase

This term designates a softer secondary phase, richer in iron than in chromium and containing very little carbon but significant amounts of silicon, i.e. 0 to 10 per cent. When viewed under the microscope, this phase is grey in colour as opposed to the chromium-rich phase which is white. This phase would be either α− or γ−(Cr,Fe) solid solution. The higher silicon values were obtained in regions where the slag had a high silica content, and the low values in regions where the slag had a correspondingly low silica content.

Carbonaceous Reducing Agent

The coke was graphitised to a considerable degree in all the samples in which it was observed. In many instances, slag had penetrated into the pores of the coke.

Once the above identification and analysis of phases had been completed, the two additional sets of electron-microprobe analyses were embarked upon.

ANALYSES OF METALLIC PHASES

The analyses of the metallic phases showed the following.

1. Near the upper surface of the furnace, metallic phases were predominantly iron-rich containing very little chromium.
2. Proceeding downwards in the furnace in the regions near the electrodes, the chromium to iron ratio in the chromium-rich phase, i.e. $(Cr,Fe)_7C_3$, increased to a maximum of about 2.5 in the metal bath itself.
3. In any one sample where there was a significant difference in the chromium to iron ratio in the chromium-rich phase, the ratio became higher as the metallic coating surrounding pieces of reducing agent increased in thickness.
4. Near the walls of the furnace at a depth corresponding to the tip of the electrodes in regions where a great deal of red spinel was found, the value of the chromium to iron ratio of chromium-rich phases in regions of coalesced metal was found to be high in general. Values of 2.5 to 7.1 were recorded.
5. The carbide $(Cr,Fe)_{23}C_6$ was encountered once in a relatively inactive zone of the furnace. This is somewhat surprising since this carbide is a phase formed at a higher temperature than $(Cr,Fe)_7C_3$. This $(Cr,Fe)_{23}C_6$ appeared within a metallic coating surrounding slag that consisted of black pyroxene and forsterite.
6. A further metallic phase was found that could not be identified. It was a very hard, grey phase with a chromium to iron ratio of approximately 1.4, and contained very little carbon and a great deal of silicon (up to 22 per cent by mass). The phase was specifically encountered in a sample from a region near the electrode under which there had been a large build-up of metal before the shut-down. The phase was a major, secondary constituent of a metallic band surrounding white PX/PL. There was no visible carbonaceous reducing agent in the sample, and the slag was very siliceous.
7. In general, the blebs within PAC particles (or in the case of type A PAC particles, the interstitial blebs) consisted of iron-rich phases. The analyses of these blebs are shown in Table III.

TABLE III
Metallic Phases Within or Associated with Specific Types of PAC Particles

Type of PAC particle	Ratios of atomic proportions Cr/Fe	C / (Cr + Fe)	Si / (Cr + Fe)	Identification of phase
A	0.01	0.0	0.00	α−(Fe,Cr) solid solution
B	0.30	0.2 → 0.3	0.00	$(Cr,Fe)_7C_3$
C	0.03 → 0.60	0.6 → 0.8	0.00	$(Cr,Fe)_7C_3$
D*				
E	0.20	0.0	0.13	α−(Fe,Cr) solid solution
F	0.06	0.1	0.10	γ−(Fe,Cr) solid solution
G	0.70	0.0	0.02	α−(Cr,Fe) solid solution
H	0.50	0.0	0.05	α−(Cr,Fe) solid solution

* No information was obtained for blebs within this type of particle.

It should be noted that the carbon values were not considered to be accurate and, therefore, they give qualitative, rather than quantitative, information. For particular phases identified by X-ray diffraction, the carbon values were lower than expected.

PROFILES OF PAC PARTICLES

Qualitative changes in the relative percentages by mass of particular cations in two different types of PAC particle can be seen from the profiles (Figs. 2 to 9). However, the quantitative changes could not be assessed without further calculation since, as certan cations are withdrawn from a crystal, there is a corresponding change in the molecular mass of that phase. To nullify this effect the atomic proportions were calculated for cations according to the analysis shown in the profile at the centre of each type of PAC particle. These are given in Table IV.

DISCUSSION

Conditions inside a furnace that has cooled over a period of months cannot be expected to be identical to conditions within a working furnace. In fact, slow cooling probably enhances the separation of some of the zones, and the formation of some of the phases in the slag and the metal. However, one can reasonably assume that many valid observations can be made.

Zones in the Furnace

The qualitative mineralogical results supported the macroscopic observations made during the dig-out of the furnace. For instance, it was clear that the active zones of the furnace are those in the region at the tips of the electrode. The relatively inactive zones are at the surface of the burden and in the region adjacent to the walls of the furnace. The red colour of samples of slag from the latter region was due to the large amount of red spinel, which was the main constituent of type H PAC particles and which contained much of the residual chromium.

The chemical analyses had already shown that residual chromium increases sideways from the tips of the electrode to the walls of the furnace and upwards to the surface of the burden. From the mineralogical observations, it was possible to ascertain that the residual chromium existed primarily within the matrices of the spinels, either primary spinels crystallized out of the slag (relatively little

TABLE IV
Atomic Proportions of Elements in Spinels at the Centre of PAC Particles when Oxygen is 4, i.e. $A^{2+}B_2^{3+}O_4$

PAC type	Mg^{2+}	Fe^{2+}	ΣA^{2+}	Al^{3+}	Cr^{3+}	Fe^{3+}	Ti^{4+}	Si^{4+}	ΣB^{3+} and B^{4+}	Total Fe	Total Cr*
A (opaque)	0,410	0,606	1,02	0,644	1,219	0,152	0,017	0	2,03	0,758	1,219
B (opaque)	0.409	0,611	1,02	0.659	1,158	0,190	0,033	0	2,04	0,801	1,158
C (opaque)	0,679	0,344	1,02	0,598	1,252	0,184	0,011	0	2,05	0,528	1,252
D (opaque)	0,903	0,148	1,05	0,524	1,156	0,424	0,006	0	2,11	0,572	1,156
E (opaque)	0,962	0,048	1,01	0,695	1,217	0,087	0,022	0,001	2,02	0,135	1,217
F (pale-pink spinel)	1,075	0	1,08	1,902	0,033	0,006	0,004	0,002	1,95	0,006	0,033
G (opaque)	1,066	0	1,07	1,215	0,708	0,014	0,014	0,005	1,96	0,014	0,708
H (light-red spinel)	0,99	0	0,99	1,855	0,141	0	0,006	0,006	2,01	0	0,141

*In the form of Cr^{3+}

of this was observed) or remnants of chromite particles. By charge balancing it was established that this chromium was in its trivalent form. Chromium may have been in its divalent form in the black, grey or green pyroxenes, but, since relatively little of these phases was observed, this would have been an insignificant amount.

Unlike chromium, residual iron was found to be mostly in the form of metallic blebs within PAC particles. All the slag phases contained negligible amounts of iron. The blebs contained some chromium, but this was generally in small amounts since the chromium to iron ratio was low (see Table III).

The general zones of the furnace that had been observed macroscopically were confirmed by the microscopic examination.

At the top of the burden was loosely sintered material, which was not examined mineralogically since little or no reaction had taken place.

In the central, active region of the furnace, the next zone down was one of incipient fusion where mostly iron oxides had been reduced. Since the almost-pure iron phases occurred only interstitially with chromite particles, it appears that the first oxides reduced were probably hematite exsolved from chrome spinel on the surface of chromite particles (this is known to happen when chromite is heated in air) and iron oxides which were constituents of the gangue minerals. It should be noted that, although the atmosphere in the body of the furnace was a reducing one, that at the surface of the burden was probably slightly oxidising.

The next step was the reduction of iron oxides within the edges of chromite spinels. In B- and C-type particles, it was optically evident that the reaction region moved from the edge of the particles towards the centre, indicating that it was a diffusion-controlled reaction, which is in agreement with the findings from a laboratory investigation (Barcza). Preferential reduction along cracks in the particles also supported this idea.

The reducing agent in this region was probably initially solid carbon in contact with the chromite particles but, once the first metallic blebs had been formed, the carbides themselves provided a route for the diffusion of carbon through metallic phases. The sintered nature of the C-type particles gives an idea of the temperature at which this degree of reduction is reached, since chromite from the Bushveld Complex sinters at about 1 300 °C.

The next zone down was the active zone consisting of slag containing E and F types of PAC particles and many

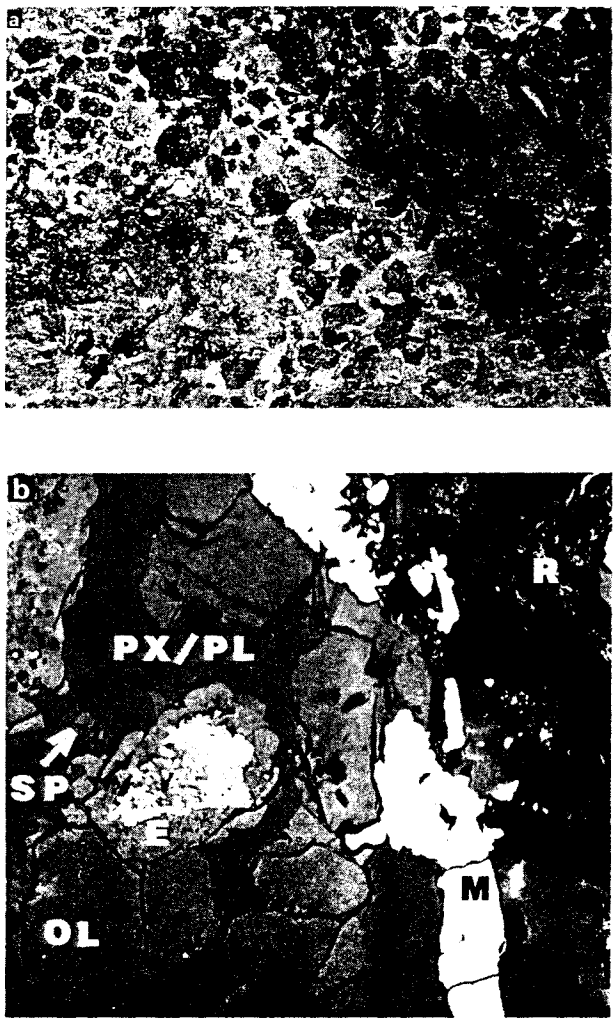

Figure 15

a. Active region of furnace showing slag (grey) and particles of carbonaceous reducing agent (black) coated with metallic phase (white).

b. Photomicrograph of a polished section of a sample from the region shown in a. The slag phases are olivine (OL), plagioclase and pyroxene (PX/PL), and a small crystal of spinel (SP). The PAC particle in the centre of the slag is E type (E). The metallic phase (M) is white and coats the reducing agent (R), which is black. Some slag is also entrained in the reducing agent. Reflected light, 200 ×. Width of figure ≡ 0,4 mm.

particles of reducing agent, each coated with a metallic layer. Fig. 15a is a photograph of this region taken during the dig-out, and Fig. 15b, shows a polished section of a sample from the same region. The metallic layer at the interface between slag and reducing medium is clearly visible.

In corresponding samples from the same level of the furnace but near the wall, comparatively few lumps of reducing agent were in evidence and, where they were observed, they were not necessarily coated with metallic phase. Coalesced metallic phases seemed very often to be independent of carbonaceous reducing medium. This may have been because the original piece of reducing agent was very small and was subsequently used up or broke away from the metallic phase. However, particularly where metallic phase encircled regions of black pyroxene and greenish forsterite, the impression gained was that carbon dissolved in slag had reduced the oxides to metal from chromium-rich phases, probably during cooling. These were the metallic phases with high chromium to iron ratios.

In some samples where slag was adjacent to chromite ore at the first stages of incipient reduction, it was observed that the amount of metallic phase in the chromite ore was most at the interface of the ore and the slag and decreased as the distance from the interface increased. This could also be an indication of carbon dissolved in the slag since there were no lumps of carbonaceous reducing agent in evidence.

Finally, at the bottom of the furnace, in the region that had been the metal bath, were solidified metallic phases with a mean chromium to iron ratio of 1.9 as shown by the chemical analysis. By means of the electron microprobe, the ratio for the chromium-rich phase in this region was found to be 2.5. The value had obviously been reduced to 1.9 as a result of dilution by iron-rich phases.

Increase of Chromium to Iron Ratio

As already mentioned, the chromium to iron ratio of chromium-rich phases was shown to increase with depth in the furnace and thickness of the metallic coatings on pieces of reducing agent. A possible explanation for this is that the first oxides reduced by the reducing agent from surrounding phases were mostly iron oxides, resulting in an iron-rich metallic coating on the reducing agent. As such a piece of reducing agent, weighted down by its metal coating, moved downwards in the furnace, it gathered more chromium-rich metallic phases by reducing the chromium oxide from the chromite, which would be richer in chromium than the chrome spinel higher in the furnace. This would be a continuous process, and it therefore could be expected that, the thicker the metallic coating on a piece of reducing agent, the richer in chromium it would be.

Order of Reduction

Table IV, which shows the atomic proportions of spinels at the centre of PAC particles at consecutive stages of reduction, is the key to the order in which the oxides that constitute the chrome spinel in local ores are reduced.

As can be seen from Table IV, the centre of particles of types A and B have a similar composition, i.e. the centres of the type B particles have not been altered. In fact, the concentration of iron in the type B particle analysed was found to be slightly higher than that of the type A particle, and this phenomenon can be attributed to statistical differences in the composition of the particles of chromite that were fed into the furnace, particularly since the furnace was fed with a mixture of ores.

After the particles have passed through stage B, iron is the first element to be withdrawn by reduction from the chromite particles. It was expected that the other elements would show increases in concentration. However, in particles at stages C and D the concentration is confined to magnesium, indicating that the charge balance in the spinel lattice and the structure of the lattice are maintained by a replacement of Fe^{2+} with Mg^{2+} ions from the surrounding gangue or flux material. This is a significant phenomenon.

Only at the stage of reduction represented by particles of type E is there a relative increase in the amount of Al^{3+} and a corresponding decrease in Fe^{3+}; the proportion of Cr^{3+} remaining very much as it was before.

From PAC particles of type E to PAC particles of type F, there is a dramatic reduction of Cr^{3+} which is accompanied by a further reduction in Fe^{3+} and a corresponding increase in Al^{3+} ions, which fill up the vacancies left by the trivalent ions. Residual chromium in the pink spinels of type F particles is 1 to 2 per cent by mass.

Optical observations show that the reduction sequence in active parts of the furnace is as described here, and is represented by the change in PAC particles from type A through B, C, D, and E to type F (sequence I). However, in less active parts of the furnace, e.g. near the sides, the reduction sequence is represented by changes in the PAC particles from type A through B, C, and D to types G and H (sequence II). The reduction of chromium from D through G to H is more gradual than that from E to F, but it is also less efficient since the residual chromium in the light-red spinels of type H is approximately 5 per cent.

The atomic proportions in Table IV show that in both sequences the order of events in the reduction of chromite from South African ores can be represented as follows:

$$\underset{\downarrow}{\overset{\text{Mg}}{}}(\text{Mg,Fe})^{2+}(\text{Cr,Al,Fe})_2^{3+}\text{O}_4 \rightarrow \text{Mg}\underset{\downarrow}{\overset{\text{Al}}{}}(\text{Cr,Al,Fe})_2^{3+}\text{O}_4 \rightarrow \text{Mg}\underset{\downarrow}{\overset{\text{Al}}{}}(\text{Cr,Al})_2^{3+}\text{O}_4.$$
$$\downarrow \qquad\qquad\qquad\qquad \downarrow \qquad\qquad\qquad\qquad \downarrow$$
$$\text{Fe}^{2+} \qquad\qquad\qquad\qquad \text{Fe}^{3+} \qquad\qquad\qquad\qquad \text{Cr}^{3+}$$

Where there is not enough aluminium to replace chromium in the last stage, the available ions would be expected to re-arrange themselves to form MgO + $MgAl_2O_4$. In fact, the spinel phase, still containing small amounts of chromium, i.e. a solid solution of $MgAl_2O_4$ (spinel) and some $MgCr_2O_4$ (picrochromite), is found in the slags, but forsterite, rather than periclase, is observed within the framework of remnant PAC particles. This forsterite must have been formed by the reaction of periclase with silica from the fluxing material.

Since the samples of slag examined had not been quenched, there would have been enough time for the following reaction to have taken place:

$$2\text{MgO} + \text{SiO}_2 \rightarrow \text{Mg}_2\text{SiO}_4.$$

The sequence of events during the reduction process as described here does not correspond to that taking place in more-refractory ores, which contain less iron and more magnesium and aluminium, than South African ores. In ores from the USSR (Kadarmetov), the order of removal of ions from the chromite lattice by reduction was found to be first Fe^{3+}, then Fe^{2+} and finally Cr^{3+}. This is the order that one would expect from crystal-field theory. However, the energies calculated on the basis of this theory are small and in this case must have only a secondary effect.

It seems that there are other conditions that control and reverse the order of the removal of divalent and trivalent iron from the chromite lattice in South African ores that have been reduced in a submerged-arc furnace. Two other conditions are suggested here.

1. The replacement of Fe^{2+} by Mg^{2+} in the chromite as the first step in the reduction process may achieve a more stable lattice, similar to that in unaltered Russian chromite, i.e. a more refractory chromite in which the

potential energy of the spinel lattice is reduced. Energy considerations would favour such a process.
2. The easy availability of magnesium ions in the gangue and flux material within the furnace means that such an ion exchange is feasible.

Alteration Sequences

The two reduction sequences as deduced from the information in Table IV are shown schematically in Fig. 16.

Fig. 17 shows the graph of cation concentration versus degree of reduction. This diagram facilitates a comparison between the nature of the reduction sequence at the end of sequence I and that at the end of sequence II.

The oscillation of the chromium values in the plateau region of this diagram is a statistical effect due to the fact that different particles were measured. The D-type particles measured was anomalous owing to the abnormally high value for Fe^{3+}.

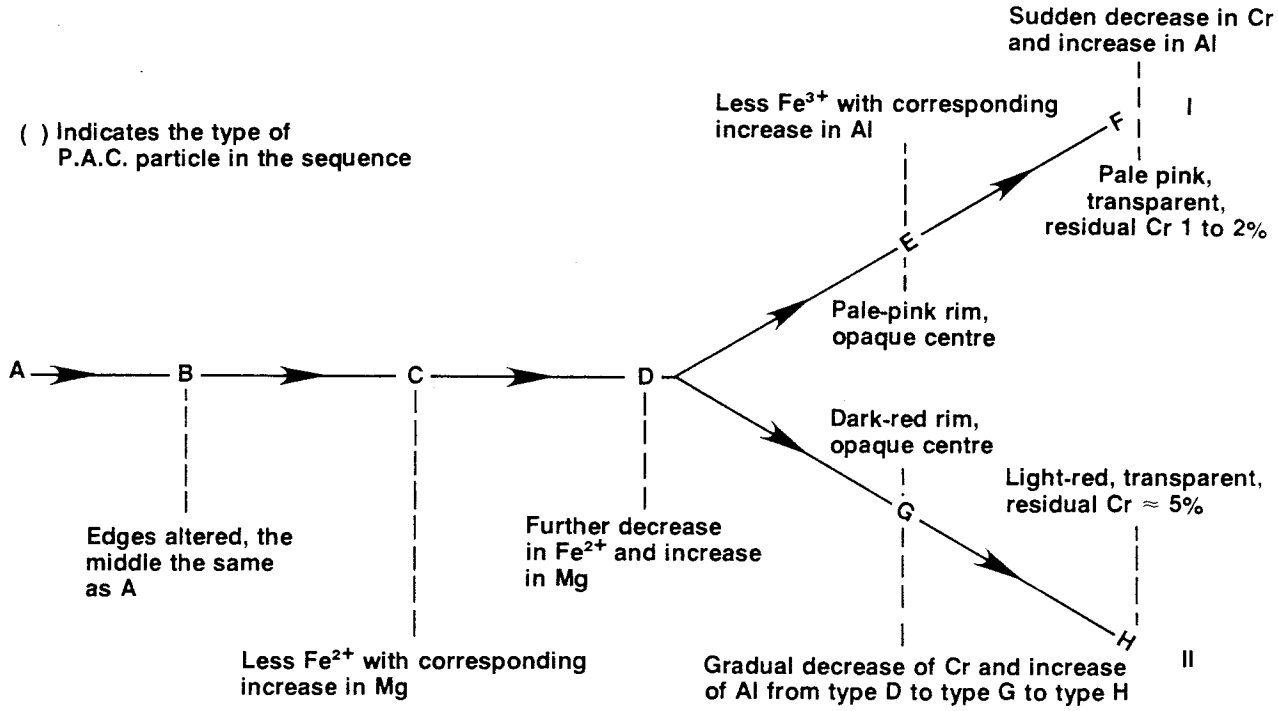

Figure 16
Diagram showing the two different alteration sequences of chromite particles.
I is typical of the sequence in active zones of the furnace.
II is typical of the sequence in less-active zones of the furnace.

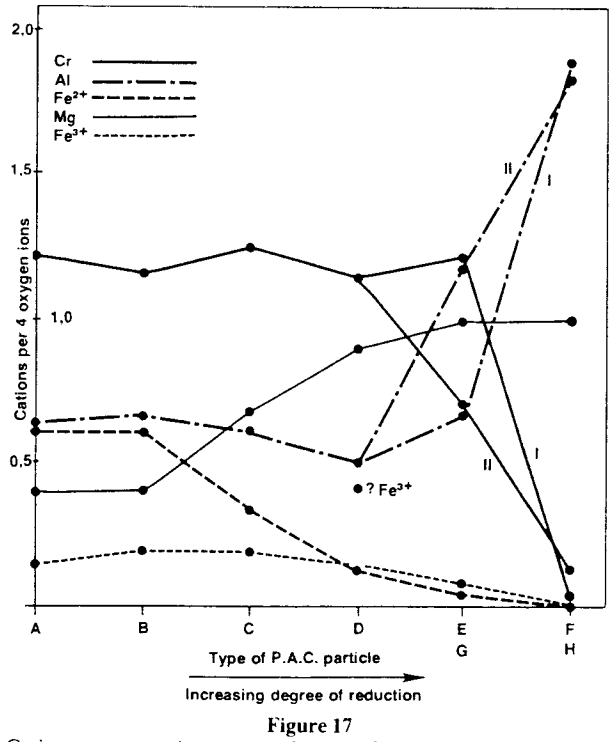

Figure 17
Cation concentration versus degree of reduction for alteration sequences I and II.

The differences between the characteristics of the alteration sequences in active and inactive zones of the furnace can be attributed in part to the lower temperatures and correspondingly lower oxygen fugacity in the inactive regions such as near the wall of the furnace. These two factors must affect the stability of chromite spinels.

There is a third variable that differs from the one type of region to the other. This is the very strong inverse correlation between the silica in the slag and the residual Cr_2O_3, as shown by the chemical analyses of samples of slag; that is, the higher the silica value, the lower the residual Cr_2O_3. (This does not apply to the residual iron.)

It is clear from the profiles that silica enters the PAC particles only at an advanced stage of alteration when most of the iron has been reduced to metallic phase. Silicon is apparent on the outer edges of type-E and type-G particles and reacts with the particles only in the final stages of reduction; that is, it reacts only with PAC particles of types F and H when forsterite, anorthite and pyroxene are found within the framework of the original chromite particles.

It is possible that a reaction between silica and chrome spinel is thermodynamically favourable at high temperatures. If so, the presence of silica contributes towards the instability of the chromite spinel and, when this happens, the reduction of Cr_2O_3 to chromium carbide takes place rapidly and efficiently.

Urquhart showed that, at 1 500 °C, when silica flux had been added to chromite ore and reducing agent, the re-

ducing process was very much more efficient. He also found that a strongly endothermic reaction took place at 1 500 °C in an experimental furnace when the charge consisted of chromite ore, reducing agent and silica. During this reaction, fumes were given off consisting of the components shown in Table V.

TABLE V
Components of Fumes

Component	%
SiO_2	55 to 60
MgO	5 to 10
Cr_2O_3	2
S as SO_4^{-2}	20 to 27
CaO	1
MnO	1

This prompted Urquhart to try to reduce chromite ore, by means of silicon monoxide only, at 1 500 °C. He found that no reduction took place except where the ore was in contact with the graphite crucible and interpreted this as meaning that silicon monoxide does not reduce chromite. However, it may be that it can reduce chromite only when carbon or some other constituent of the reducing agent, e.g. sulphur, is also present.

In the early stages of reduction of chromite in both the active and the inactive zone of a furnace, carbon diffuses into the chromite particle and acts as a reducing agent. However, it seems that there are two reduction processes taking place at 1 500 °C. The first is a continuation of the reduction by carbon either directly or by carbon dissolved in metallic phases. The second process is due to silica promoting the breakdown of chrome spinels to permit the dissolution of some chromium and iron into the slag and, thus, to facilitate the subsequent reduction of the oxides of chromium and iron by solid carbon in the form of coke particles within the slag, and possibly by some carbon actually dispersed throughout the slag phases, as indicated by some of the observations made during this investigation.

In the active regions, the second process probably predominates in the final stages of reduction, resulting in efficient and vigorous removal of chromium from the spinel lattices.

In less-active zones, the former reduction process predominates, resulting in a more gradual and less complete removal of chromium from the chromite lattice.

Silicon in Metallic Phases

From Table IV it can be seen that silicon was found only in blebs within PAC particles that were near the end of the reduction process and that the amount of silicon was considerably higher in the PAC particles of types E and F than in types G and H.

In general, it appeared that the silicon content of the metallic phases (usually α- or γ-(Fe,Cr) solid solutions) was proportional to the concentration or activity of silica in the surrounding slag. The control of silicon in the metal is important if the required metal specification is to be met. The above relationship between silicon and silica is, therefore, an important factor in the smelting behaviour of the raw materials in this process.

CONCLUSIONS

Dr E.J. Oosthuyzen is currently carrying out a project at NIM, to assess quantitatively, using an image analyser, the amount of residual chromium in the various phases in samples of slag tapped from a ferrochromium furnace. Possible hosts for this residual chromium are metallic blebs, primary spinel that crystallized out of the slags, and PAC particles.

If the greatest amount of residual chromium is found in these particles, which, from the present study seems possible, it will indicate that the loss of efficiency in the whole ferrochromium process is primarily due to incomplete reduction of chrome spinel.

If this is so, the conclusion reached in the present work regarding the sequence of events in the reduction of chrome spinel could have far-reaching results, especially the effect of replacements of Fe^{2+} by Mg^{2+}, and of Cr^{3+} by Al^{3+}, on the overall stability of the spinel. Such solid-state substitutions could, for instance, influence decisions regarding the recipe to be used in the production of composite briquettes consisting of ore, reducing agent and fluxing material. The utilisation of chromite fines will probably necessitate an ever-increasing use of briquettes, and their components should be chosen so as to maximise the efficiency of the reduction process.

ACKNOWLEDGMENTS

Grateful acknowledgment is made to the staff of Ferrometals and to Samancor Management Services for their invaluable assistance and contributions to this dig-out, and also to the NIM dig-out team led by N.A. Barcza: H.G. Griessel, J.P.R. de Villiers, M. Summers, D. Parsons and C.L. Shepstone.

Grateful thanks are also due to E.A. Viljoen and J.A. Russell of NIM for the many electron-microprobe analyses which were an essential feature of this work, and also to senior colleagues in the Mineralogy Division at NIM for useful discussion and advice, particularly Drs S.A. Hiemstra and S.A. de Waal.

This paper is presented by permission of NIM.

REFERENCES

BARCZA, N.A. (1971). *Incipient fusion studies in the system chromite-CaO-MgO-Al_2O_3-SiO_2-C.* M.Sc.(Eng.) thesis (unpubl.), University of the Witwatersrand, Johannesburg, 178 pp.

DE WAAL, S.A. (1972). The interrelation of the chemical, physical, and certain metallurgical properties of chrome spinels from the Bushveld Igneous Complex. *Rept. Nat. Inst. Metall.*, Johannesburg, No. 1415, 80 pp.

GRIFFING, N.R., FORGENG, W.D., and HEALY, G.W. (1962). C-Cr-Fe liquidus surface. *Trans. Metall. Soc., Amer. Inst. Min. Engng.*, vol. 224, pp. 148–159.

KADARMETOV, K.N. (1975). Slag formation during the reduction of lump chromium ore. *Izv. vyssk. ucheb. Zaved. Cher. Metall.*, vol. 18, No. 6, pp. 31–36.

NEUFVILLE, J.D., and SCHAIRER, J.F. (1962). The joint diopside-Ca Tschermak molecule at atmospheric pressure. *Carnegie Inst. Washington Yrbk.*, vol. 61, pp. 56–59.

SOMMER, G. (1979). The Cancer Project: a summary of computer-aided operation of a 48 MVA ferrochromium furnace. *Rept. Nat. Inst. Metall.*, Randburg, No. 2032, 22 pp.

URQUHART, R. (1972). *A study of the production of high-carbon ferrochromium in the submerged-arc furnace.* Ph.D.(Eng.) thesis (unpubl.), University of the Witwatersrand, Johannesburg, 213 pp.

WEDEPOHL, A., and BARCZA, N.A. (1981). The observations made during the dig-out of a 48 MVA ferrochromium furnace. *Rept. Nat. Inst. Metall.*, Randburg, No. 2090, 61 pp.

WETHMAR, J.C.M. (1972). Phase equilibria in the Cr-Fe-Si-C system in the composition range representative of high-carbon ferrochromium alloys produced in South Africa. *Rept. Nat. Inst. Metall.*, Johannesburg, No. 1457, 11 pp.